PROCEEDINGS OF SCIENCE

Depth of maximum of air-shower profiles at the Pierre Auger Observatory: Measurements above $10^{17.2}$ eV and Composition Implications

Jose Bellido[*,a] **for the Pierre Auger Collaboration**[b]

[a] *The University of Adelaide, School of Physical Sciences, South Australia, 5005, Australia*
[b] *Observatory Pierre Auger, Av. San Martín Norte 304, 5613 Malargüe, Argentina*
E-mail: auger_spokespersons@fnal.gov
Full author list: http://www.auger.org/archive/authors_icrc_2017.html

We present distributions of shower depth of maximum ($X_{\rm max}$) and their interpretation in terms of the cosmic ray mass composition. The measurements of $X_{\rm max}$ are based on data from the fluorescence telescopes of the Pierre Auger Observatory. Due to the extension of the field of view with the High Elevation Auger Telescopes, a lower energy threshold of $10^{17.2}$ eV can be reached. At the highest energies we have increased the available statistics by including three more years of data in the analysis compared to our previous publications. We present estimates of the first two moments of the $X_{\rm max}$ distribution and of the composition fractions over a large energy range, from $10^{17.2}$ eV to about $10^{19.6}$ eV. The composition fractions are estimated by fitting the $X_{\rm max}$ distributions with four elemental groups represented by p, He, N and Fe and using post-LHC hadronic models.

35th International Cosmic Ray Conference -ICRC2017-
10-20 July, 2017
Bexco, Busan, Korea

*Speaker.

PoS(ICRC2017)506

1. Introduction

Knowledge of the composition of cosmic rays in the energy range of 0.1 to 1 EeV is the key to identifying a possible transition from galactic to extra-galactic sources and for understanding the nature of features in the energy spectrum, such as the "ankle" (at ≈ 4 EeV) and the flux suppression (the differential flux falls to one-half of the value of the power-law extrapolation at 4×10^{19} eV [1]).

The atmospheric depth at which the energy deposited by the Extensive Air Shower (EAS) reaches its maximum, $X_{\max}$, is one of the most robust observables for studying the mass composition. Experimentally, the longitudinal profile of the shower development can be measured using fluorescence light emitted by molecules of atmospheric nitrogen excited by EAS particles. At the Pierre Auger Observatory, which has taken data continuously since 01.2004, such measurements are performed using the fluorescence detector (FD) consisting of 24 telescopes placed at 4 locations and, since 06.2010, using the High Elevation Auger Telescopes (HEAT). The HEAT telescopes have expanded the field of view (FoV) of the Coihueco site (CO) from $2^\circ \div 30^\circ$ up to $2^\circ \div 60^\circ$ in elevation, which allows one to observe nearby low energy showers ($E < 10^{17.8}$ eV). In the following, we refer to the HEAT/CO system as HeCo.

In Fig. 1 an example of a low energy event in the enlarged FoV is shown: the track on the camera (left) and the longitudinal profile with the Gaisser-Hillas fit (right).

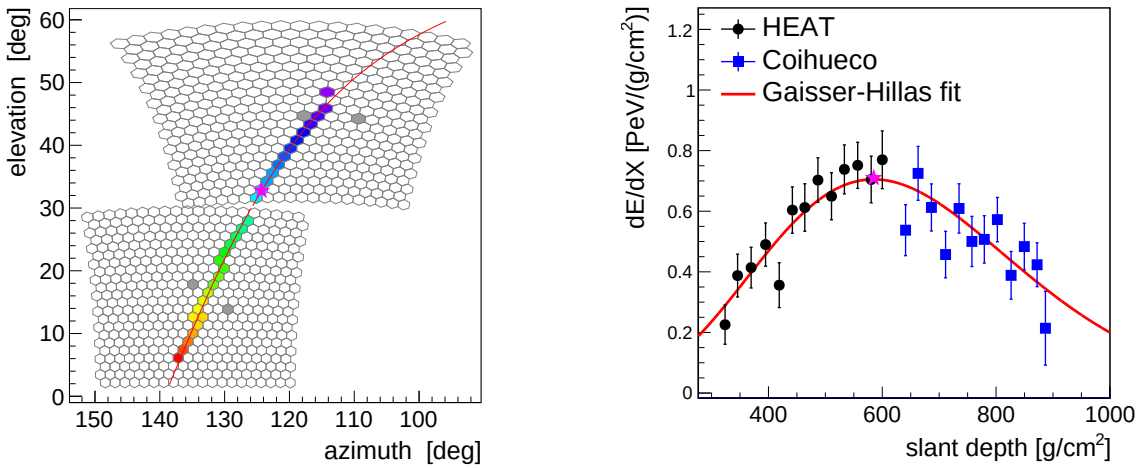

Figure 1: Example of a HeCo event with an energy of $(4.7 \pm 0.2) \times 10^{17}$ eV. Left: the camera view with the timing of the pixel pulses color-coded (early = blue, late = red). Right: the measured longitudinal profile (black circles — HEAT, blue squares — Coihueco) with the Gaisser-Hillas fit (red line). The magenta star in both panels indicates the $X_{\max}$ position.

In this paper, over five years of calibrated HEAT data, from 01.06.2010 to 31.12.2015, are used to extend the previous measurement of the $X_{\max}$ distributions [2] from $10^{17.8}$ eV down to $10^{17.2}$ eV. In addition, at the highest energies we have increased the available statistics by including data from three more years in the analysis compared to [2].

In estimating the unbiased $X_{\max}$ distributions and their corresponding first two moments, we have followed an identical procedure to that in a previous publication [2]. Most of the systematic uncertainties estimated in [2] for the standard fluorescence detectors (Standard-FD) are also valid

for the HEAT/Coihueco (HeCo) $X_{\max}$ analysis. So for further details of the $X_{\max}$ analysis and of most of the systematic studies we refer the reader to [2].

The determination of the primary composition is performed by comparing the measured $X_{\max}$ distributions of EAS with expectations according to high energy hadronic interaction models [3]. The first two moments of the $X_{\max}$ distribution ($\langle X_{\max}\rangle$ and $\sigma(X_{\max})$) are related to the first two moments of the distribution of the logarithm of masses of primary particles ($\ln A$ and $\sigma(\ln A)$) [4]:

$$\langle X_{\max}\rangle = \langle X_{\max}\rangle_p + f_E\langle \ln A\rangle \tag{1.1}$$

$$\sigma^2(X_{\max}) = \langle \sigma^2_{\rm sh}\rangle + f_E^2\,\sigma^2(\ln A). \tag{1.2}$$

$\langle X_{\max}\rangle_p$ and $\langle \sigma^2_{\rm sh}\rangle$ are the mean $X_{\max}$ for protons and the composition-averaged shower-to-shower fluctuations, and f_E is a parameter depending on details of hadronic interactions, properly parametrized from the interaction models for energies $\geq 10^{17}$ eV.

2. Data analysis

The analysis presented in this paper is based on two statistically independent datasets. These are the data collected by the Standard-FD telescopes (during the period from 01.12.2004 to 31.12.2015), and the data collected with HeCo (during the period from 01.06.2010 to 31.12.2015). The events with energies below $10^{18.1}$ eV recorded by CO telescopes during periods where HEAT telescopes were in operation are considered in the HeCo dataset (even if they do not include any HEAT telescope). Otherwise, they are considered in the Standard-FD telescope dataset. So, the Standard-FD dataset contains events with energies above $10^{17.8}$ eV and the HeCo dataset contains events with energies between $10^{17.2}$ eV and $10^{18.1}$ eV.

HEAT can be operated in upward and downward modes. The downward mode is when the telescopes are oriented such that their elevation angle extends up to 30°. The upward mode is when they cover an elevation angle ranging from 30° to 60° (this is the HEAT standard operation mode). The HEAT downward mode is used for systematic cross checks, because it allows one to observe the same showers in coincidence with telescopes from the Coihueco site.

There have been some updates in the energy and $X_{\max}$ scale. These changes arose from improvements in the reconstruction of the shower profile (mainly affecting lower energy events) and improvements in the estimate of the vertical atmospheric optical depth [5].

2.1 Data selection

The analysis is based on hybrid events, i.e. on events with geometries reconstructed using information on arrival times of both light in the cameras of FD telescopes and of the shower front at ground as measured by the surface station closest to the shower axis. We selected data recorded during stable running conditions and good atmospheric conditions [2]. In addition to these selection criteria a set of fiducial FoV cuts are applied to reduce to a minimum the detector effects in the sampled $X_{\max}$ distributions (as explained in Section 2.2).

2.2 FoV selection criteria

A shower is reconstructed accurately only if its $X_{\max}$ is within the detector FoV. Shallow or deep events are more likely to have their $X_{\max}$ values outside the FoV and be excluded from the analysis. In general, at lower energies where the showers are closer to the telescopes, the limited FoV biases the sample towards lighter composition (i.e. towards deeper $X_{\max}$ values).

For data satisfying the selection criteria explained in Section 2.1, a fiducial FoV is derived. This fiducial range is characterized by the lower X_{low} and upper X_{up} boundaries. These parameters define the slant depth range where $X_{\max}$ of each event would be reconstructed with a resolution better than 40 g cm^{-2}. To have higher quality events, the $X_{\max}$ value must fall inside these boundaries. Furthermore, if the values of X_{low} and X_{up} are not within certain limits (i.e. X_{low} and X_{up} should enclose the bulk of the $X_{\max}$ distribution), the event is also excluded. The processes to calculate the X_{low} and X_{up} parameters, and the limits on them, are explained in detail in [2].

2.3 Estimating the $X_{\max}$ moments

After the application of all selection criteria, the moments of the $X_{\max}$ distribution are estimated as described in [2]. Small energy and $X_{\max}$ reconstruction biases are estimated through simulations and corrected for. The observed width of the distribution is corrected by subtracting the detector resolution (Fig. 2, left) in quadrature to obtain $\sigma(X_{\max})$. The $X_{\max}$ resolution worsens at lower energies because the average length of the observed profiles (in g/cm^2) decreases at lower energies. The step between the HeCo and the Standard-FD resolution is because the $X_{\max}$ reconstruction of events involving HEAT and Coihueco telescopes is very sensitive to small differences in the energy calibration of the HEAT and Coihueco telescopes. Inter-telescope calibration fluctuations with time have widened the sampled $X_{\max}$ distributions. We correct for this detector effect by increasing the detector resolution for HeCo. The $\langle X_{\max} \rangle$ fluctuations as a function of time are evaluated to determine how much the resolution should be increased.

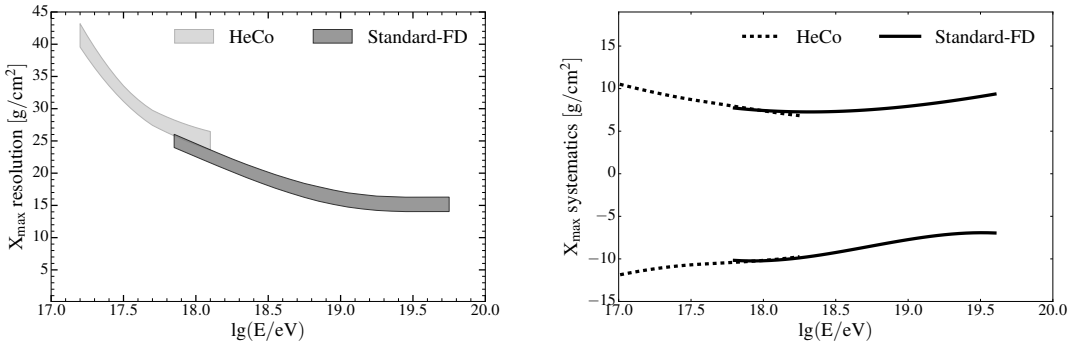

Figure 2: Left: $X_{\max}$ resolution as a function of energy for the HeCo and the Standard-FD datasets. Right: Systematic uncertainties in the $X_{\max}$ scale as a function of energy.

The systematic uncertainty in the $X_{\max}$ scale is displayed in Fig. 2 (right). At low energies it is dominated by uncertainties in the analysis procedure, while at high energies atmospheric uncertainties also contribute.

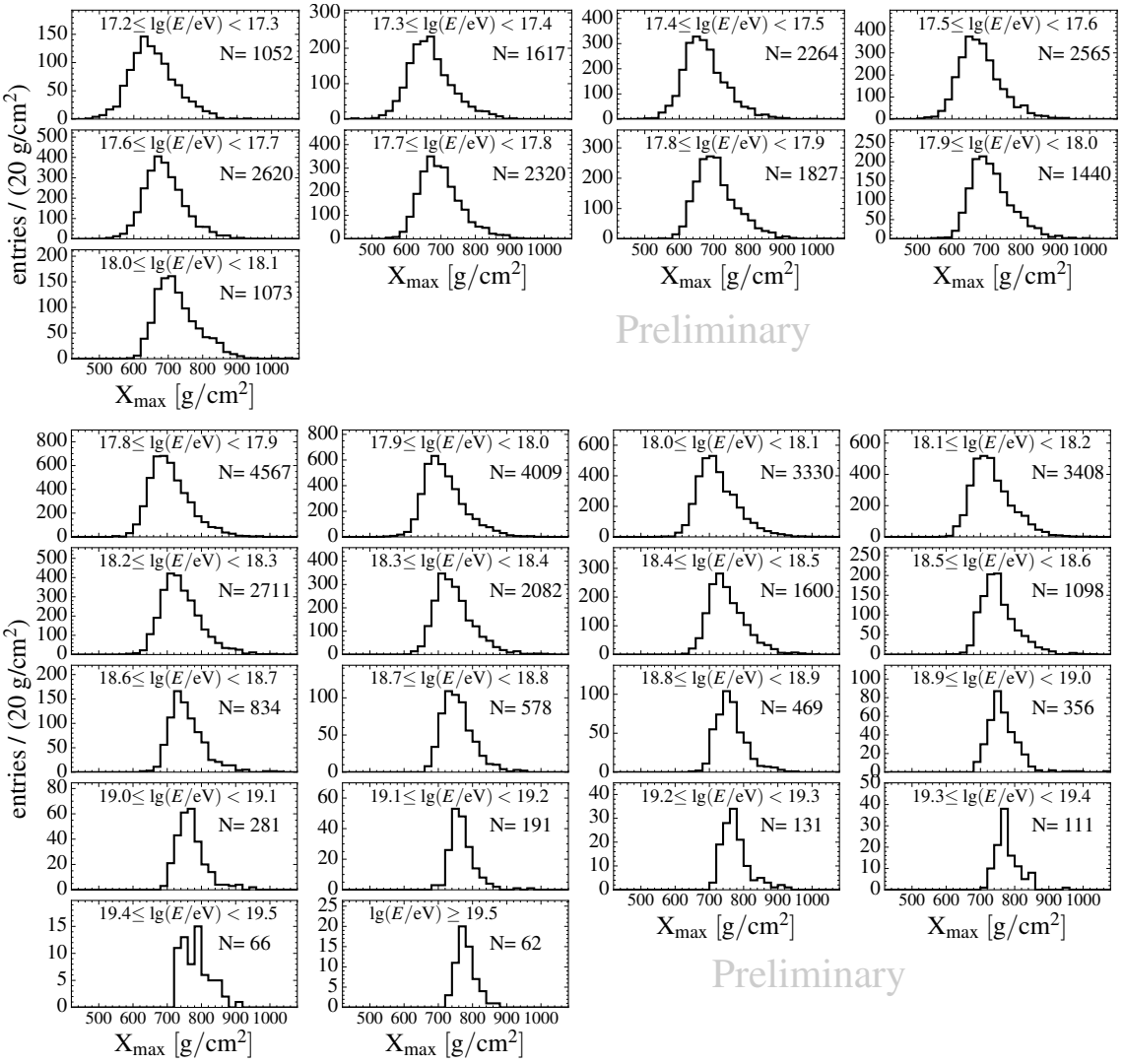

Figure 3: $X_{\max}$ distributions for different energy intervals from the HeCo (top) and Standard-FD (bottom) datasets. The number of events in each energy bin is indicated.

2.4 Results and Interpretation

We present the results of the HeCo and the Standard-FD $X_{\max}$ distributions in energy bins of $\Delta\lg(E/\text{eV}) = 0.1$ extending from $10^{17.2}$ eV to $10^{18.1}$ eV for HeCo and above $10^{17.8}$ eV for the Standard-FD telescopes. The $X_{\max}$ distributions after applying quality and fiducial selection cuts are shown in Fig. 3. These distributions still include effects of the detector resolution and the detector acceptance. The total number of events that passed all cuts (quality and FoV cuts) is 16778 and 25884 for HeCo and Standard-FD respectively.

The $\langle X_{\max}\rangle$ difference between HeCo and the Standard-FD datasets is on average $\sim$2.3 g/cm^2 for overlapping energy bins. This small offset is within the uncorrelated systematics of the two analyses. Consequently, for the combination of the datasets the HeCo $\langle X_{\max}\rangle$ is shifted accordingly and the resulting $\langle X_{\max}\rangle$ and $\sigma(X_{\max})$ as a function of energy are shown in Fig. 4. These $X_{\max}$

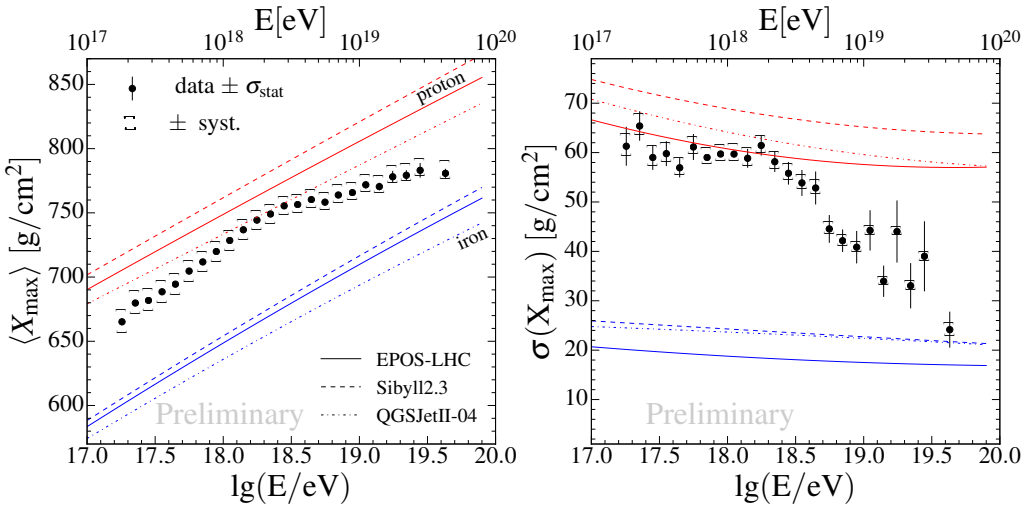

Figure 4: The mean (left) and the standard deviation (right) of the measured $X_{\max}$ distributions as a function of energy compared to air-shower simulations for proton and iron primaries.

moments are in good agreement with those in our previous publications [6, 2] and they can be compared directly with expectations from hadronic models. These is because we have removed all detector effects, such as the detector resolution and the non homogeneous $X_{\max}$ acceptance within the tails of the $X_{\max}$ distributions.

Between $10^{17.2}$ and $10^{18.33}$ eV the observed elongation rate (rate of change of $\langle X_{\max} \rangle$) is (80 ± 1) g/cm^2/decade (Fig. 4, left). This value, being larger than that expected for a constant mass composition (~ 60 g/cm^2/decade), indicates that the mean primary mass is becoming lighter with increasing energy. At $10^{18.32 \pm 0.02}$ eV the elongation rate becomes significantly smaller ((26 ± 2) g/cm^2/decade) indicating that the composition is becoming heavier with increasing energy. The fluctuations of $X_{\max}$ (Fig. 4, right) decrease above $10^{18.3}$ eV, also indicating a composition becoming heavier with increasing energy.

The mean value of $\ln A$, $\langle \ln A \rangle$, and its variance, $\sigma^2(\ln A)$, determined from Eqs. (1.1) and (1.2), are shown in Fig. 5. For the parameters $\langle X_{\max} \rangle_p$, f_E and $\langle \sigma^2_{sh} \rangle$, the EPOS-LHC [7], QGSJetII-04 [8] and Sibyll2.3 [9] hadronic interaction models are used. The unphysical negative values obtained for $\sigma^2(\ln A)$ result from the corresponding hadronic model predicting $\sigma(X_{\max})$ values (for pure compositions) that are larger than the observed ones. An average value of $\sigma^2(\ln A) \simeq 1.2 - 2.6$ has been estimated in [10] using the correlation between $X_{\max}$ and S_{1000} (the signal recorded at 1000 m). This range for $\sigma^2(\ln A)$ is valid for the three hadronic models and for the energy range $\lg(E/\text{eV}) = 18.5 - 19.0$. The average $\sigma^2(\ln A)$ from Fig. 5, for the same energy range, is (0.8 ± 0.4) for EPOS-LHC, (-0.7 ± 0.4) for QGSJetII-04, (0.6 ± 0.4) for Sibyll2.3. The QGSJetII-04 and Sibyll2.3 models failed to provide consistent interpretation, and EPOS-LHC is marginally consistent.

For the three models, similar trends with energy for $\langle \ln A \rangle$ and $\sigma^2(\ln A)$ are observed. The primary mass is decreasing with energy reaching minimum values at $10^{18.32 \pm 0.02}$ eV, and then it starts to increase again towards higher energies. The spread of the masses is almost constant until $\approx 10^{18.3}$ eV after which it starts to decrease. Together with the behavior of $\langle \ln A \rangle$, this is an indication that the relative fraction of protons becomes smaller for energies above $\approx 10^{18.3}$ eV.

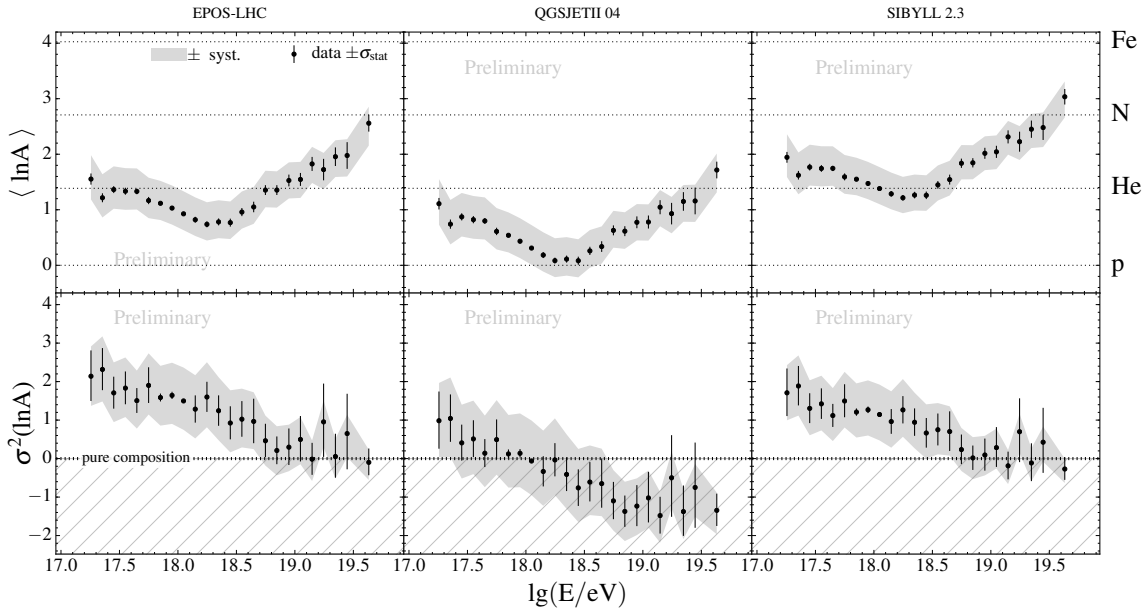

Figure 5: The mean (top) and the variance (bottom) of ln$A$ estimated from data with EPOS-LHC (left), QGSJetII-04 (middle) and Sibyll2.3 (right) hadronic interaction models.

The expected $X_{\max}$ distributions for p, He, N and Fe have been parametrized [11] using a gaussian convolution with an exponential function according to the hadronic models (EPOS-LHC, QGSJetII-04 and Sibyll2.3) using CONEX [12]. These parametrization have been used to fit for the fraction of p, He, N and Fe in each energy bin. The corresponding detector resolution and acceptance (for each energy bin) have been considered in the fits. Fig. 6 shows the fit fractions as a function of energy for the three different models. The panel at the bottom indicates the goodness of the fits (p-values). The trend of the He and N fractions as a function of energy has a strong dependence on the particular hadronic model used. However, the three hadronic models agree when estimating a null Fe abundance between $10^{18.3}$ eV and $10^{19.4}$ eV.

This interpretation of the cosmic ray composition as a function of energy relies on the validity of the hadronic interaction models. The p-values estimated in Fig. 6 provide an indication on how well the models managed to reproduced the observed $X_{\max}$ distributions with the fractions fit. For good fits, the p-values should be randomly distributed between 0 and 1, and should not be too small. A large fraction of the p-values shown in Fig. 6 (bottom panel) are below the 0.1 line, but we only expect 10% of p-values to be below this line. There is a total of 24 energy bins, so we expect in average 2.4 p-values below the 0.1 line, but we observe 8 (for EPOS-LHC), 11 (for Sibyll2.3), and 17 (for QGSJetII-04). The large fraction of small p-values indicates that the models were not able to find combinations of fractions to reproduce the details of the observed $X_{\max}$ distribution.

References

[1] P. L. Ghia, *Highlights from the Pierre Auger Observatory*, PoS(ICRC2015)034, 2016.

[2] A. Aab *et al.*, *Depth of maximum of air-shower profiles at the Pierre Auger Observatory. I. Measurements at energies above* $10^{17.8}$ *eV*, *Phys. Rev.* **D90, no. 12** (122005), 2014.

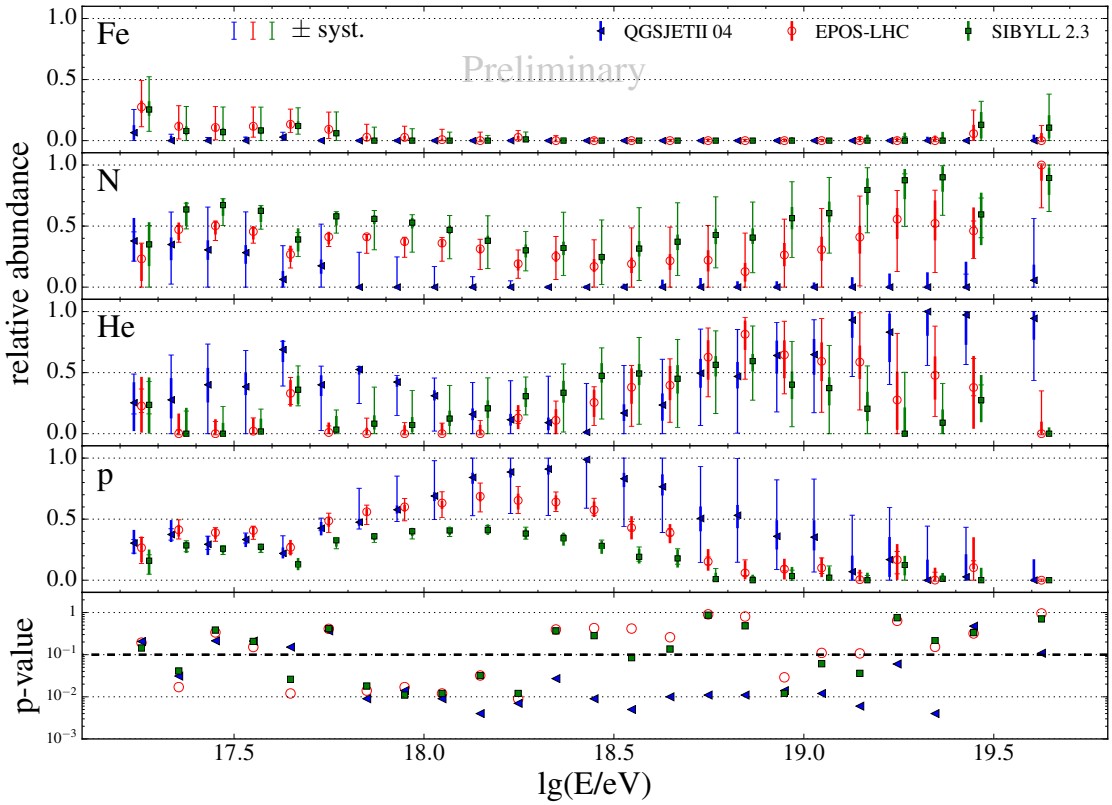

Figure 6: Mass fraction fits obtained using parametrizations of the expected X_{max} distributions using the HeCo and the Standard-FD X_{max} data. The error bars indicate the statistics (smaller cap) and the systematic uncertainties (larger cap). The bottom panel indicates the goodness of the fits (p-values).

[3] A. Aab *et al.*, *Depth of maximum of air-shower profiles at the Pierre Auger Observatory. II. Composition implications*, *Phys. Rev.* **D90, no. 12** (122006), 2014.

[4] P. Abreu *et al.*, *Interpretation of the Depths of Maximum of Extensive Air Showers Measured by the Pierre Auger Observatory*, *JCAP* **1302** (026), 2013.

[5] M. Malacari et al. [Pierre Auger Collaboration]. Proc. 35nd ICRC (2017), this conference.

[6] J. Abraham *et al.*, *Measurement of the Depth of Maximum of Extensive Air Showers above* 10^{18} *eV*, *Phys. Rev. Lett.* **104** (091101), 2010.

[7] T. Pierog and K. Werner *Phys. Rev. Lett.* **101** (171101), 2008.

[8] S. Ostapchenko *Phys. Rev.* **D83** (014018), 2011.

[9] F. Riehn, R. Engel, A. Fedynitch, T. K. Gaisser, and T. Stanev, *A new version of the event generator Sibyll*, PoS(ICRC2015)558, 2016.

[10] A. Aab *et al.*, *Evidence for a mixed mass composition at the "ankle" in the cosmic-ray spectrum*, *Phys. Lett.* **B762** (288), 2016.

[11] S. Blaess, J. Bellido, B. Dawson, PoS(ICRC2017)490, 2017.

[12] T. Bergmann et al. *Astropart. Phys.* **26** (420), 2007.

The Pierre Auger Collaboration

A. Aab[77], P. Abreu[69], M. Aglietta[50,49], I.F.M. Albuquerque[18], I. Allekotte[1], A. Almela[8,11], J. Alvarez Castillo[65], J. Alvarez-Muñiz[76], G.A. Anastasi[41,43], L. Anchordoqui[83], B. Andrada[8], S. Andringa[69], C. Aramo[47], N. Arsene[71], H. Asorey[1,27], P. Assis[69], J. Aublin[32], G. Avila[9,10], A.M. Badescu[72], A. Balaceanu[70], F. Barbato[57], R.J. Barreira Luz[69], K.H. Becker[34], J.A. Bellido[12], C. Berat[33], M.E. Bertaina[59,49], X. Bertou[1], P.L. Biermann[b], J. Biteau[31], S.G. Blaess[12], A. Blanco[69], J. Blazek[29], C. Bleve[53,45], M. Boháčová[29], D. Boncioli[43,g], C. Bonifazi[24], N. Borodai[66], A.M. Botti[8,36], J. Brack[f], I. Brancus[70], T. Bretz[38], A. Bridgeman[35], F.L. Briechle[38], P. Buchholz[40], A. Bueno[75], S. Buitink[77], M. Buscemi[55,44], K.S. Caballero-Mora[63], B. Caccianiga[46], L. Caccianiga[56], A. Cancio[11,8], F. Canfora[77], L. Caramete[71], R. Caruso[55,44], A. Castellina[50,49], F. Catalani[16], G. Cataldi[45], L. Cazon[69], A.G. Chavez[64], J.A. Chinellato[19], J. Chudoba[29], R.W. Clay[12], A. Cobos[8], R. Colalillo[57,47], A. Coleman[87], L. Collica[49], M.R. Coluccia[53,45], R. Conceição[69], G. Consolati[46], G. Consolati[46,51], F. Contreras[9,10], M.J. Cooper[12], S. Coutu[87], C.E. Covault[81], J. Cronin[88], S. D'Amico[52,45], B. Daniel[19], S. Dasso[5,3], K. Daumiller[36], B.R. Dawson[12], R.M. de Almeida[26], S.J. de Jong[77,79], G. De Mauro[77], J.R.T. de Mello Neto[24,25], I. De Mitri[53,45], J. de Oliveira[26], V. de Souza[17], J. Debatin[35], O. Deligny[31], M.L. Díaz Castro[19], F. Diogo[69], C. Dobrigkeit[19], J.C. D'Olivo[65], Q. Dorosti[40], R.C. dos Anjos[23], M.T. Dova[4], A. Dundovic[39], J. Ebr[29], R. Engel[36], M. Erdmann[38], M. Erfani[40], C.O. Escobar[e], J. Espadanal[69], A. Etchegoyen[8,11], H. Falcke[77,80,79], J. Farmer[88], G. Farrar[85], A.C. Fauth[19], N. Fazzini[e], F. Fenu[59,49], B. Fick[84], J.M. Figueira[8], A. Filipčič[74,73], M.M. Freire[6], T. Fujii[88], A. Fuster[8,11], R. Gaïor[32], B. García[7], F. Gaté[d], H. Gemmeke[37], A. Gherghel-Lascu[70], U. Giaccari[24], M. Giammarchi[46], M. Giller[67], D. Głas[68], C. Glaser[38], G. Golup[1], M. Gómez Berisso[1], P.F. Gómez Vitale[9,10], N. González[8,36], A. Gorgi[50,49], A.F. Grillo[43], T.D. Grubb[12], F. Guarino[57,47], G.P. Guedes[20], R. Halliday[81], M.R. Hampel[8], P. Hansen[4], D. Harari[1], T.A. Harrison[12], A. Haungs[36], T. Hebbeker[38], D. Heck[36], P. Heimann[40], A.E. Herve[35], G.C. Hill[12], C. Hojvat[e], E. Holt[36,8], P. Homola[66], J.R. Hörandel[77,79], P. Horvath[30], M. Hrabovský[30], T. Huege[36], J. Hulsman[8,36], A. Insolia[55,44], P.G. Isar[71], I. Jandt[34], J.A. Johnsen[82], M. Josebachuili[8], J. Jurysek[29], A. Kääpä[34], O. Kambeitz[35], K.H. Kampert[34], B. Keilhauer[36], N. Kemmerich[18], E. Kemp[19], J. Kemp[38], R.M. Kieckhafer[84], H.O. Klages[36], M. Kleifges[37], J. Kleinfeller[9], R. Krause[38], N. Krohm[34], D. Kuempel[34], G. Kukec Mezek[73], N. Kunka[37], A. Kuotb Awad[35], B.L. Lago[15], D. LaHurd[81], R.G. Lang[17], M. Lauscher[38], R. Legumina[67], M.A. Leigui de Oliveira[22], A. Letessier-Selvon[32], I. Lhenry-Yvon[31], K. Link[35], D. Lo Presti[55], L. Lopes[69], R. López[60], A. López Casado[76], R. Lorek[81], Q. Luce[31], A. Lucero[8,11], M. Malacari[88], M. Mallamaci[56,46], D. Mandat[29], P. Mantsch[e], A.G. Mariazzi[4], I.C. Mariş[13], G. Marsella[53,45], D. Martello[53,45], H. Martinez[61], O. Martínez Bravo[60], J.J. Masías Meza[3], H.J. Mathes[36], S. Mathys[34], G. Matthiae[58,48], E. Mayotte[34], P.O. Mazur[e], C. Medina[82], G. Medina-Tanco[65], D. Melo[8], A. Menshikov[37], K.-D. Merenda[82], S. Michal[30], M.I. Micheletti[6], L. Middendorf[38], L. Miramonti[56,46], B. Mitrica[70], D. Mockler[35], S. Mollerach[1], F. Montanet[33], C. Morello[50,49], G. Morlino[41,43], M. Mostafá[87], A.L. Müller[8,36], G. Müller[38], M.A. Muller[19,21], S. Müller[35,8], R. Mussa[49], I. Naranjo[1], L. Nellen[65], P.H. Nguyen[12], M. Niculescu-Oglinzanu[70], M. Niechciol[40], L. Niemietz[34], T. Niggemann[38], D. Nitz[84], D. Nosek[28], V. Novotny[28], L. Nožka[30], L.A. Núñez[27], L. Ochilo[40], F. Oikonomou[87], A. Olinto[88], M. Palatka[29], J. Pallotta[2], P. Papenbreer[34], G. Parente[76], A. Parra[60], T. Paul[83], M. Pech[29], F. Pedreira[76], J. Pękala[66], R. Pelayo[62], J. Peña-Rodriguez[27], L. A. S. Pereira[19], M. Perlin[8], L. Perrone[53,45], C. Peters[38], S. Petrera[41,43], J. Phuntsok[87], R. Piegaia[3], T. Pierog[36], M. Pimenta[69], V. Pirronello[55,44], M. Platino[8], M. Plum[38], J. Poh[88], C. Porowski[66], R.R. Prado[17], P. Privitera[88], M. Prouza[29], E.J. Quel[2], S. Querchfeld[34], S. Quinn[81], R. Ramos-Pollan[27], J. Rautenberg[34], D. Ravignani[8], J. Ridky[29], F. Riehn[69], M. Risse[40], P. Ristori[2], V. Rizi[54,43], W. Rodrigues de Carvalho[18], G. Rodriguez Fernandez[58,48], J. Rodriguez Rojo[9], M.J. Roncoroni[8], M. Roth[36], E. Roulet[1], A.C. Rovero[5], P. Ruehl[40], S.J. Saffi[12], A. Saftoiu[70],

F. Salamida[54,43], H. Salazar[60], A. Saleh[73], G. Salina[48], F. Sánchez[8], P. Sanchez-Lucas[75], E.M. Santos[18], E. Santos[8], F. Sarazin[82], R. Sarmento[69], C. Sarmiento-Cano[8], R. Sato[9], M. Schauer[34], V. Scherini[45], H. Schieler[36], M. Schimp[34], D. Schmidt[36,8], O. Scholten[78,c], P. Schovánek[29], F.G. Schröder[36], S. Schröder[34], A. Schulz[35], J. Schumacher[38], S.J. Sciutto[4], A. Segreto[42,44], R.C. Shellard[14], G. Sigl[39], G. Silli[8,36], R. Šmída[36], G.R. Snow[89], P. Sommers[87], S. Sonntag[40], J. F. Soriano[83], R. Squartini[9], D. Stanca[70], S. Stanič[73], J. Stasielak[66], P. Stassi[33], M. Stolpovskiy[33], F. Strafella[53,45], A. Streich[35], F. Suarez[8,11], M. Suarez Durán[27], T. Sudholz[12], T. Suomijärvi[31], A.D. Supanitsky[5], J. Šupík[30], J. Swain[86], Z. Szadkowski[68], A. Taboada[36], O.A. Taborda[1], V.M. Theodoro[19], C. Timmermans[79,77], C.J. Todero Peixoto[16], L. Tomankova[36], B. Tomé[69], G. Torralba Elipe[76], P. Travnicek[29], M. Trini[73], R. Ulrich[36], M. Unger[36], M. Urban[38], J.F. Valdés Galicia[65], I. Valiño[76], L. Valore[57,47], G. van Aar[77], P. van Bodegom[12], A.M. van den Berg[78], A. van Vliet[77], E. Varela[60], B. Vargas Cárdenas[65], R.A. Vázquez[76], D. Veberič[36], C. Ventura[25], I.D. Vergara Quispe[4], V. Verzi[48], J. Vicha[29], L. Villaseñor[64], S. Vorobiov[73], H. Wahlberg[4], O. Wainberg[8,11], D. Walz[38], A.A. Watson[a], M. Weber[37], A. Weindl[36], M. Wiedeński[68], L. Wiencke[82], H. Wilczyński[66], T. Winchen[34], M. Wirtz[38], D. Wittkowski[34], B. Wundheiler[8], L. Yang[73], A. Yushkov[8], E. Zas[76], D. Zavrtanik[73,74], M. Zavrtanik[74,73], A. Zepeda[61], B. Zimmermann[37], M. Ziolkowski[40], Z. Zong[31], F. Zuccarello[55,44]

—•—

[1] Centro Atómico Bariloche and Instituto Balseiro (CNEA-UNCuyo-CONICET), San Carlos de Bariloche, Argentina
[2] Centro de Investigaciones en Láseres y Aplicaciones, CITEDEF and CONICET, Villa Martelli, Argentina
[3] Departamento de Física and Departamento de Ciencias de la Atmósfera y los Océanos, FCEyN, Universidad de Buenos Aires and CONICET, Buenos Aires, Argentina
[4] IFLP, Universidad Nacional de La Plata and CONICET, La Plata, Argentina
[5] Instituto de Astronomía y Física del Espacio (IAFE, CONICET-UBA), Buenos Aires, Argentina
[6] Instituto de Física de Rosario (IFIR) - CONICET/U.N.R. and Facultad de Ciencias Bioquímicas y Farmacéuticas U.N.R., Rosario, Argentina
[7] Instituto de Tecnologías en Detección y Astropartículas (CNEA, CONICET, UNSAM), and Universidad Tecnológica Nacional - Facultad Regional Mendoza (CONICET/CNEA), Mendoza, Argentina
[8] Instituto de Tecnologías en Detección y Astropartículas (CNEA, CONICET, UNSAM), Buenos Aires, Argentina
[9] Observatorio Pierre Auger, Malargüe, Argentina
[10] Observatorio Pierre Auger and Comisión Nacional de Energía Atómica, Malargüe, Argentina
[11] Universidad Tecnológica Nacional - Facultad Regional Buenos Aires, Buenos Aires, Argentina
[12] University of Adelaide, Adelaide, S.A., Australia
[13] Université Libre de Bruxelles (ULB), Brussels, Belgium
[14] Centro Brasileiro de Pesquisas Fisicas, Rio de Janeiro, RJ, Brazil
[15] Centro Federal de Educação Tecnológica Celso Suckow da Fonseca, Nova Friburgo, Brazil
[16] Universidade de São Paulo, Escola de Engenharia de Lorena, Lorena, SP, Brazil
[17] Universidade de São Paulo, Instituto de Física de São Carlos, São Carlos, SP, Brazil
[18] Universidade de São Paulo, Instituto de Física, São Paulo, SP, Brazil
[19] Universidade Estadual de Campinas, IFGW, Campinas, SP, Brazil
[20] Universidade Estadual de Feira de Santana, Feira de Santana, Brazil
[21] Universidade Federal de Pelotas, Pelotas, RS, Brazil
[22] Universidade Federal do ABC, Santo André, SP, Brazil
[23] Universidade Federal do Paraná, Setor Palotina, Palotina, Brazil
[24] Universidade Federal do Rio de Janeiro, Instituto de Física, Rio de Janeiro, RJ, Brazil
[25] Universidade Federal do Rio de Janeiro (UFRJ), Observatório do Valongo, Rio de Janeiro, RJ, Brazil

[26] Universidade Federal Fluminense, EEIMVR, Volta Redonda, RJ, Brazil
[27] Universidad Industrial de Santander, Bucaramanga, Colombia
[28] Charles University, Faculty of Mathematics and Physics, Institute of Particle and Nuclear Physics, Prague, Czech Republic
[29] Institute of Physics of the Czech Academy of Sciences, Prague, Czech Republic
[30] Palacky University, RCPTM, Olomouc, Czech Republic
[31] Institut de Physique Nucléaire d'Orsay (IPNO), Université Paris-Sud, Univ. Paris/Saclay, CNRS-IN2P3, Orsay, France
[32] Laboratoire de Physique Nucléaire et de Hautes Energies (LPNHE), Universités Paris 6 et Paris 7, CNRS-IN2P3, Paris, France
[33] Laboratoire de Physique Subatomique et de Cosmologie (LPSC), Université Grenoble-Alpes, CNRS/IN2P3, Grenoble, France
[34] Bergische Universität Wuppertal, Department of Physics, Wuppertal, Germany
[35] Karlsruhe Institute of Technology, Institut für Experimentelle Kernphysik (IEKP), Karlsruhe, Germany
[36] Karlsruhe Institute of Technology, Institut für Kernphysik, Karlsruhe, Germany
[37] Karlsruhe Institute of Technology, Institut für Prozessdatenverarbeitung und Elektronik, Karlsruhe, Germany
[38] RWTH Aachen University, III. Physikalisches Institut A, Aachen, Germany
[39] Universität Hamburg, II. Institut für Theoretische Physik, Hamburg, Germany
[40] Universität Siegen, Fachbereich 7 Physik - Experimentelle Teilchenphysik, Siegen, Germany
[41] Gran Sasso Science Institute (INFN), L'Aquila, Italy
[42] INAF - Istituto di Astrofisica Spaziale e Fisica Cosmica di Palermo, Palermo, Italy
[43] INFN Laboratori Nazionali del Gran Sasso, Assergi (L'Aquila), Italy
[44] INFN, Sezione di Catania, Catania, Italy
[45] INFN, Sezione di Lecce, Lecce, Italy
[46] INFN, Sezione di Milano, Milano, Italy
[47] INFN, Sezione di Napoli, Napoli, Italy
[48] INFN, Sezione di Roma "Tor Vergata", Roma, Italy
[49] INFN, Sezione di Torino, Torino, Italy
[50] Osservatorio Astrofisico di Torino (INAF), Torino, Italy
[51] Politecnico di Milano, Dipartimento di Scienze e Tecnologie Aerospaziali , Milano, Italy
[52] Università del Salento, Dipartimento di Ingegneria, Lecce, Italy
[53] Università del Salento, Dipartimento di Matematica e Fisica “E. De Giorgi”, Lecce, Italy
[54] Università dell'Aquila, Dipartimento di Scienze Fisiche e Chimiche, L'Aquila, Italy
[55] Università di Catania, Dipartimento di Fisica e Astronomia, Catania, Italy
[56] Università di Milano, Dipartimento di Fisica, Milano, Italy
[57] Università di Napoli "Federico II", Dipartimento di Fisica “Ettore Pancini“, Napoli, Italy
[58] Università di Roma “Tor Vergata”, Dipartimento di Fisica, Roma, Italy
[59] Università Torino, Dipartimento di Fisica, Torino, Italy
[60] Benemérita Universidad Autónoma de Puebla, Puebla, México
[61] Centro de Investigación y de Estudios Avanzados del IPN (CINVESTAV), México, D.F., México
[62] Unidad Profesional Interdisciplinaria en Ingeniería y Tecnologías Avanzadas del Instituto Politécnico Nacional (UPIITA-IPN), México, D.F., México
[63] Universidad Autónoma de Chiapas, Tuxtla Gutiérrez, Chiapas, México
[64] Universidad Michoacana de San Nicolás de Hidalgo, Morelia, Michoacán, México
[65] Universidad Nacional Autónoma de México, México, D.F., México
[66] Institute of Nuclear Physics PAN, Krakow, Poland
[67] University of Łódź, Faculty of Astrophysics, Łódź, Poland

[68] University of Łódź, Faculty of High-Energy Astrophysics,Łódź, Poland
[69] Laboratório de Instrumentação e Física Experimental de Partículas - LIP and Instituto Superior Técnico - IST, Universidade de Lisboa - UL, Lisboa, Portugal
[70] "Horia Hulubei" National Institute for Physics and Nuclear Engineering, Bucharest-Magurele, Romania
[71] Institute of Space Science, Bucharest-Magurele, Romania
[72] University Politehnica of Bucharest, Bucharest, Romania
[73] Center for Astrophysics and Cosmology (CAC), University of Nova Gorica, Nova Gorica, Slovenia
[74] Experimental Particle Physics Department, J. Stefan Institute, Ljubljana, Slovenia
[75] Universidad de Granada and C.A.F.P.E., Granada, Spain
[76] Universidad de Santiago de Compostela, Santiago de Compostela, Spain
[77] IMAPP, Radboud University Nijmegen, Nijmegen, The Netherlands
[78] KVI - Center for Advanced Radiation Technology, University of Groningen, Groningen, The Netherlands
[79] Nationaal Instituut voor Kernfysica en Hoge Energie Fysica (NIKHEF), Science Park, Amsterdam, The Netherlands
[80] Stichting Astronomisch Onderzoek in Nederland (ASTRON), Dwingeloo, The Netherlands
[81] Case Western Reserve University, Cleveland, OH, USA
[82] Colorado School of Mines, Golden, CO, USA
[83] Department of Physics and Astronomy, Lehman College, City University of New York, Bronx, NY, USA
[84] Michigan Technological University, Houghton, MI, USA
[85] New York University, New York, NY, USA
[86] Northeastern University, Boston, MA, USA
[87] Pennsylvania State University, University Park, PA, USA
[88] University of Chicago, Enrico Fermi Institute, Chicago, IL, USA
[89] University of Nebraska, Lincoln, NE, USA

———

[a] School of Physics and Astronomy, University of Leeds, Leeds, United Kingdom
[b] Max-Planck-Institut für Radioastronomie, Bonn, Germany
[c] also at Vrije Universiteit Brussels, Brussels, Belgium
[d] SUBATECH, École des Mines de Nantes, CNRS-IN2P3, Université de Nantes, France
[e] Fermi National Accelerator Laboratory, USA
[f] Colorado State University, Fort Collins, CO
[g] now at Deutsches Elektronen-Synchrotron (DESY), Zeuthen, Germany

Acknowledgments

The successful installation, commissioning, and operation of the Pierre Auger Observatory would not have been possible without the strong commitment and effort from the technical and administrative staff in Malargüe. We are very grateful to the following agencies and organizations for financial support:

Argentina – Comisión Nacional de Energía Atómica; Agencia Nacional de Promoción Científica y Tecnológica (ANPCyT); Consejo Nacional de Investigaciones Científicas y Técnicas (CONICET); Gobierno de la Provincia de Mendoza; Municipalidad de Malargüe; NDM Holdings and Valle Las Leñas; in gratitude for their continuing cooperation over land access; Australia – the Australian Research Council; Brazil – Conselho Nacional de Desenvolvimento Científico e Tecnológico (CNPq); Financiadora de Estudos e Projetos (FINEP); Fundação de Amparo à Pesquisa do Estado de Rio de Janeiro (FAPERJ); São Paulo Research Foundation (FAPESP) Grants No. 2010/07359-6 and No. 1999/05404-3; Ministério de Ciência e Tecnologia (MCT); Czech Republic – Grant No. MSMT CR LG15014, LO1305, LM2015038 and CZ.02.1.01/0.0/0.0/16_013/0001402; France – Centre de Calcul IN2P3/CNRS; Centre National de la Recherche Scientifique (CNRS); Conseil Régional Ile-de-France; Département Physique Nucléaire et Corpusculaire (PNC-IN2P3/CNRS); Département Sciences de l'Univers (SDU-INSU/CNRS); Institut Lagrange de Paris (ILP) Grant No. LABEX ANR-10-LABX-63 within the Investissements d'Avenir

Programme Grant No. ANR-11-IDEX-0004-02; Germany – Bundesministerium für Bildung und Forschung (BMBF); Deutsche Forschungsgemeinschaft (DFG); Finanzministerium Baden-Württemberg; Helmholtz Alliance for Astroparticle Physics (HAP); Helmholtz-Gemeinschaft Deutscher Forschungszentren (HGF); Ministerium für Innovation, Wissenschaft und Forschung des Landes Nordrhein-Westfalen; Ministerium für Wissenschaft, Forschung und Kunst des Landes Baden-Württemberg; Italy – Istituto Nazionale di Fisica Nucleare (INFN); Istituto Nazionale di Astrofisica (INAF); Ministero dell'Istruzione, dell'Universitá e della Ricerca (MIUR); CETEMPS Center of Excellence; Ministero degli Affari Esteri (MAE); Mexico – Consejo Nacional de Ciencia y Tecnología (CONACYT) No. 167733; Universidad Nacional Autónoma de México (UNAM); PAPIIT DGAPA-UNAM; The Netherlands – Ministerie van Onderwijs, Cultuur en Wetenschap; Nederlandse Organisatie voor Wetenschappelijk Onderzoek (NWO); Stichting voor Fundamenteel Onderzoek der Materie (FOM); Poland – National Centre for Research and Development, Grants No. ERA-NET-ASPERA/01/11 and No. ERA-NET-ASPERA/02/11; National Science Centre, Grants No. 2013/08/M/ST9/00322, No. 2013/08/M/ST9/00728 and No. HARMONIA 5–2013/10/M/ST9/00062, UMO-2016/22/M/ST9/00198; Portugal – Portuguese national funds and FEDER funds within Programa Operacional Factores de Competitividade through Fundação para a Ciência e a Tecnologia (COMPETE); Romania – Romanian Authority for Scientific Research ANCS; CNDI-UEFISCDI partnership projects Grants No. 20/2012 and No. 194/2012 and PN 16 42 01 02; Slovenia – Slovenian Research Agency; Spain – Comunidad de Madrid; Fondo Europeo de Desarrollo Regional (FEDER) funds; Ministerio de Economía y Competitividad; Xunta de Galicia; European Community 7th Framework Program Grant No. FP7-PEOPLE-2012-IEF-328826; USA – Department of Energy, Contracts No. DE-AC02-07CH11359, No. DE-FR02-04ER41300, No. DE-FG02-99ER41107 and No. DE-SC0011689; National Science Foundation, Grant No. 0450696; The Grainger Foundation; Marie Curie-IRSES/EPLANET; European Particle Physics Latin American Network; European Union 7th Framework Program, Grant No. PIRSES-2009-GA-246806; European Union's Horizon 2020 research and innovation programme (Grant No. 646623); and UNESCO.

Last modified on 2017-07-31.